REGULAR PAPER

Soliton solutions and self-steepening in the photon-conserving nonlinear Schrödinger equation

S. M. Hernandez[a], J. Bonetti[b,c], N. Linale[b,c], D. F. Grosz[b,c], and P. I. Fierens[c,d]

[a]Instituto Balseiro, Universidad Nacional de Cuyo, Bariloche, Río Negro 8400, Argentina;
[b]Depto. de Ingeniería en Telecomunicaciones, Centro Atómico Bariloche, Comisión Nacional de Energía Atómica, Río Negro 8400, Argentina;
[c]Consejo Nacional de Investigaciones Científicas y Técnicas (CONICET), Argentina;
[d]Centro de Optoelectrónica, Instituto Tecnológico de Buenos Aires (ITBA), CABA 1106, Argentina

ARTICLE HISTORY
Compiled December 9, 2020

ABSTRACT
We have recently introduced a new modeling equation for the propagation of pulses in optical waveguides, the photon-conserving Nonlinear Schrödinger Equation (pc-NLSE) which, unlike the canonical NLSE, guarantees strict conservation of both the energy and the number of photons for any arbitrary frequency-dependent nonlinearity. In this paper we analyze some properties of this new equation in the familiar case where the nonlinear coefficient of the waveguide does not change sign. We show that the pcNLSE effectively adds a correction term to the NLSE proportional to the deviation of the self-steepening (SS) parameter from the photon-conserving condition in the NLSE. Furthermore, we describe the role of the self-steepening parameter in the context of the conservation of the number of photons, and derive an analytical expression for the relation of the SS parameter with the time delay experienced by pulses upon propagation. Finally, we put forth soliton-like solutions of the pcNLSE that, unlike NLSE solitons, conserve the number of photons for any arbitrary SS parameter.

KEYWORDS
Nonlinear optics; nonlinear Schrödinger equation; soliton; self-steepening; photon number

1. Introduction

The nonlinear Schrödinger equation (NLSE) is widespread used to model propagation of light pulses in nonlinear Kerr media, such as nonlinear optical fibers and waveguides. Derived as an approximation based on the Maxwell equations [1], it has proven to be accurate in a wide variety of cases. It also has been extended to include other nonlinear effects such as the stimulated Raman scattering. Nonetheless, the NLSE and some of its generalizations may well reach the limits of their validity in various scenarios as, for instance, in few-cycle pulses [2–9].

Modifications of the NLSE are also needed in the case of waveguides with a frequency-dependent nonlinearity [10–16]. Interest on this type of waveguides has in-

CONTACT S. M. Hernandez. Email: shernandez@ib.edu.ar

creased with the introduction of new kinds of materials, such as nanoparticle-doped glasses [17–28], silicon photonic nanowires [29,30], and other metamaterials [13,14,31–34]. The nonlinear refractive index in these media is strongly frequency dependent, giving rise to unusual phenomena such as solitons and modulation instability in the normal-dispersion regime, the existence of a zero-nonlinearity wavelength, and even a controllable self-steepening (SS) parameter [13,27]. Although the NLSE can be straightforwardly modified to account for a wavelength dependence in the nonlinear coefficient, it is a well-established fact that, in general, *this approach does not preserve neither the energy nor the photon number* [15,35,36].

By means of quantum mechanical considerations and a generalized Miller's rule [37], we have recently introduced a photon-conserving nonlinear Schrödinger equation (pc-NLSE) [38] that accounts for the frequency dependence of the nonlinearity without the perils of producing unphysical results, such as an increase in the number of photons along propagation. We have shown that this new equation can be used to model modulation instability in materials exhibiting zero-nonlinearity wavelengths [39,40] and two-photon absorption [41]. We also have further extended this new modeling equation to incorporate stimulated Raman scattering [42].

In this work, we focus on applications of the pcNLSE to the usual case where the nonlinear coefficient of the medium does not change sign. In particular, we explore the propagation of certain types of pulses, including a first step into the existence analysis of soliton-like waves. This study not only enlightens our understanding of this new equation, but it also opens up the path to experimental applications such as the measurement of the frequency-dependent nonlinearity. The remaining of the paper is organized as follows. In Section 2 we review the pcNLSE, develop an approximation for narrowband pulses that gives a deeper insight into this new equation, and derive an expression for the relation between the pulse delay experienced along propagation and the self-steepening parameter which may be used to measure this important waveguide parameter. Section 3 is devoted to soliton-like pulses under the pcNLSE, where we first present a simple type of solitons for a particular value of the self-steepening parameter, and then extend results to other values of this parameter focusing on narrowband pulses. Finally, we summarize our results and discuss lines of future research in Section 4.

2. Photon-conserving NLSE

For the sake of reference, let us describe the nonlinear Schrödinger equation which is customarily used to model the propagation of pulses in optical waveguides. In the frequency domain, the NLSE can be written as [1]

$$\frac{\partial \tilde{A}(z,\Omega)}{\partial z} = i\tilde{\beta}(\Omega)\tilde{A} + i\gamma(\Omega)\mathcal{F}\left\{A(z,t)|A(z,t)|^2\right\}, \tag{1}$$

where $\tilde{A}(z,\Omega)$ is the Fourier transform of the pulse complex envelope $A(z,t)$ and Ω is the deviation from a conveniently chosen reference frequency ω_0. $\tilde{\beta}(\Omega)$ and $\tilde{\gamma}(\Omega)$ model the linear dispersion and the nonlinearity of the waveguide, respectively. It is

usual to work with the series expansions

$$\tilde{\beta}(\Omega) = \frac{1}{2}\beta_2\Omega^2 + \frac{1}{3!}\beta_3\Omega^3 + \cdots, \tag{2}$$

$$\tilde{\gamma}(\Omega) = \gamma_0 + \gamma_1\Omega + \frac{1}{2}\gamma_2\Omega^2 + \cdots \tag{3}$$

Given that we are interested in lossless/gainless waveguides, we assume that $\beta_k, \gamma_k \in \mathbb{R}$. It must be noted that we do not include β_1 in the expansion of $\tilde{\beta}(\Omega)$ as we assume, as it is customary, that time in Eq. (1) is measured with respect to a moving frame with velocity β_1^{-1}.

In many real applications it is sufficient to use only first order expansions of $\tilde{\gamma}(\Omega)$ [43], and we focus on this case in this paper. Oftentimes, the following linear relation is used

$$\tilde{\gamma}(\Omega) = \gamma_0 + \frac{\gamma_0}{\omega_0}\Omega. \tag{4}$$

As it is explained in Ref. [36], this is the only frequency dependence of the nonlinearity that preserves the number of photons in the NLSE. However, it has been observed that this relation cannot adequately account for pulse propagation in every circumstance, even in cases where $\tilde{\gamma}(\Omega)$ does not change sign in the spectral region of interest [44]. Since we want to depart from this situation, in the remaining of this work we assume that

$$\tilde{\gamma}(\Omega) = \gamma_0 + s\frac{\gamma_0}{\omega_0}\Omega, \tag{5}$$

where $s \in \mathbb{R}$ can be either positive or negative depending on the particular propagation medium being considered, and is a measure of the deviation from the NLSE photon-conserving scenario.

As already mentioned, we have recently introduced a photon-conserving nonlinear Schrödinger equation which, based on a simple quantum-mechanical picture of four-wave-mixing interactions and a generalized Miller's rule [38], allows for the modeling of arbitrary frequency-dependent nonlinear profiles. The pcNLSE in the frequency domain reads

$$\frac{\partial\tilde{A}}{\partial z} = i\tilde{\beta}(\Omega)\tilde{A} + i\Gamma(\Omega)\mathcal{F}\left(C^*B^2\right) + i\Gamma^*(\Omega)\mathcal{F}\left(B^*C^2\right), \tag{6}$$

where

$$\tilde{B}(z,\Omega) = \sqrt[4]{\frac{\tilde{\gamma}(\Omega)}{\omega_0+\Omega}}\tilde{A}(z,\Omega), \tag{7}$$

$$\tilde{C}(z,\Omega) = \left(\sqrt[4]{\frac{\tilde{\gamma}(\Omega)}{\omega_0+\Omega}}\right)^*\tilde{A}(z,\Omega), \tag{8}$$

$$\Gamma(\Omega) = \frac{1}{2}\sqrt[4]{\tilde{\gamma}(\Omega)(\omega_0+\Omega)^3}, \tag{9}$$

where M^* is the complex conjugate of M. As it may be expected, the pcNLSE agrees

with the NLSE in the case where the latter conserves the number of photons, i.e., when $s = 1$. In spite of its apparent complexity, the pcNLSE can be efficiently solved by the same numerical tools as the NLSE, such as the Split-Step Fourier algorithm [1]. It has been shown that this new equation can model the modulation instability phenomenon in materials exhibiting zero-nonlinearity wavelengths (ZNWs), where the NLSE fails to conserve such a basic physical quantity as the photon number. Reference [39] shows that the NLSE and the pcNLSE predict very different modulation-instability gain profiles, especially when the spectral region of interest includes a ZNW. The pcNLSE has also been successfully applied to the analysis of waveguides doped with metal nanoparticles [40], and a modified pcNLSE has been used to model two-photon absorption [41] and stimulated Raman scattering [42]. This latter extension has enabled methods to analyze higher-order nonlinearities in waveguides, [45].

In the particular case where $\tilde{\gamma}(\Omega)$ does not change sign, Eq. (6) can be simplified. For the sake of simplicity, we assume that $\gamma_0 > 0$, although results can be easily generalized. Under this scenario, $\tilde{B} = \tilde{C}$ and $\Gamma(\Omega) \in \mathbb{R}$. The pcNLSE can thus be written as

$$\frac{\partial \tilde{A}}{\partial z} = i\tilde{\beta}(\Omega)\tilde{A} + i\sqrt[4]{(\omega_0+\Omega)\tilde{\gamma}(\Omega)}\mathcal{F}\left\{B|B|^2\right\}. \tag{10}$$

Furthermore, we may express this equation in terms only of $B(z,t)$:

$$\frac{\partial \tilde{B}}{\partial z} = i\tilde{\beta}(\Omega)\tilde{B} + i\sqrt{(\omega_0+\Omega)\tilde{\gamma}(\Omega)}\mathcal{F}\left\{B|B|^2\right\}. \tag{11}$$

Note that this equation is formally equivalent to Eq. (1). This observation allows us to use results present in the large body of literature on the NLSE, a trick we resort to in Section 3. Moreover, this similarity between the NLSE and the pcNLSE in terms of the pulse envelope A and the B field, respectively, may help researchers in the area to better understand the implications of this new modeling equation.

2.1. Approximation for spectrally narrow wavepackets

The self-steepening parameter s is related to the shock-wave formation in optical pulses under the NLSE [1], and this is also the case for the photon-conserving NLSE. In this section, we describe the role of the SS parameter in the pcNLSE with the aid of an approximation for narrowband pulses.

Let us assume that the frequency content of the propagating wave is narrow such that $|\tilde{A}(\Omega)|$ is negligible unless $|\Omega| \ll \omega_0$. In this case, introducing Eq. (5) in Eq. (11) and using a Taylor expansion to a first order in Ω/ω_0, we may approximate the pcNLSE as

$$\frac{\partial A}{\partial z} \approx i\hat{\beta}A + i\gamma_0\left(1 + i\frac{1}{\omega_0}\frac{\partial}{\partial t}\right)\left(A|A|^2\right) - \gamma_0\left(\frac{s-1}{\omega_0}\right)|A|^2\frac{\partial A}{\partial t}, \tag{12}$$

where $\hat{\beta}$ is the operator in the time domain corresponding to $\tilde{\beta}(\Omega)$ (details of these calculations can be found in Appendix A.) As expected, Eq. (12) gives back the NLSE when $s = 1$, i.e., the only case where the NLSE conserves the number of photons.

Moreover, Eq. (12) allows us to regard the pcNLSE, for spectrally narrow wavepackets, as introducing a correction to the NLSE given by the last term.

Equation (12) also helps us comprehend the role of the self-steepening parameter s. We take a first step in this understanding by analyzing the important case of $s = -2$. For the sake of simplicity, let us assume that there is no linear dispersion, i.e., $\tilde{\beta}(\Omega) = 0$. Some simple calculations (see Appendix B) show that Eq. (12) reduces to

$$\frac{\partial A(z,t)}{\partial z} = i\gamma_0 A|A|^2 + \frac{\gamma_0}{\omega_0} A \left(A^* \frac{\partial A}{\partial t} - A \frac{\partial A^*}{\partial t} \right), \tag{13}$$

where we have changed the approximation for an equality. It is interesting to observe that the factor in parenthesis in the second term is proportional to the squared amplitude times the instantaneous frequency of $A(z,t)$. Furthermore, it can be easily shown that $\partial_z |A|^2 = 0$ (see Appendix B). Remarkably, this implies that solutions to Eq. (13) do not exhibit the effect of self-steepening which might be expected from the introduction of the linear dependence of $\gamma(\Omega)$ in Eq. (5) (see Chapter 4 in Ref. [1]) and that pulse shape is preserved along propagation.

Although these conclusions were derived under an approximation to the pcNLSE for narrowband pulses, simulation results show their predictions to be correct. Indeed, Fig. 1 shows simulation results using Eq. (6), assuming no approximations, for the propagation of a 100-fs Gaussian pulse with peak power $P_0 = 10$ kW and central wavelength $\lambda_0 = 1550$ nm. The pulse is propagated 1.5 km along a waveguide with $\gamma_0 = 1\ \mathrm{W^{-1}\,km^{-1}}$ and no linear dispersion, i.e., $\beta_k = 0$. As it can be observed, there is evidence of the formation of an optical shock for values of $s \neq -2$. However, for $s = -2$ there is no significant change in the pulse shape even after such a long propagated distance.

2.2. Nonlinearity-dependent time delay

A deeper understanding of the role of the self-steepening in the pcNLSE can be gained by turning to quasi-analytical solutions of Eq. (12). The method of moments (see, e.g., Refs. [46,47]) is a powerful tool to find this type of solutions. Let us write

$$A(z,t) = \sqrt{P_0}\rho\left(\frac{t-T}{T_0}\right) \exp\left(-iC_p \frac{(t-T)^2}{2T_0^2}\right), \tag{14}$$

where $\rho(\tau)$ is the pulse shape, P_0 is the pulse power, T the time delay, C_p the pulse chirp, and we have assumed that the pulse width T_0 does not change significantly along propagation.

Let us focus on the time delay, which may be calculated as the weighted average

$$T(z) = \frac{1}{E} \int_{-\infty}^{+\infty} t|A(t,z)|^2 dt, \tag{15}$$

where E is the pulse energy defined by

$$E = \int_{-\infty}^{+\infty} |A(t,z)|^2 dt. \tag{16}$$

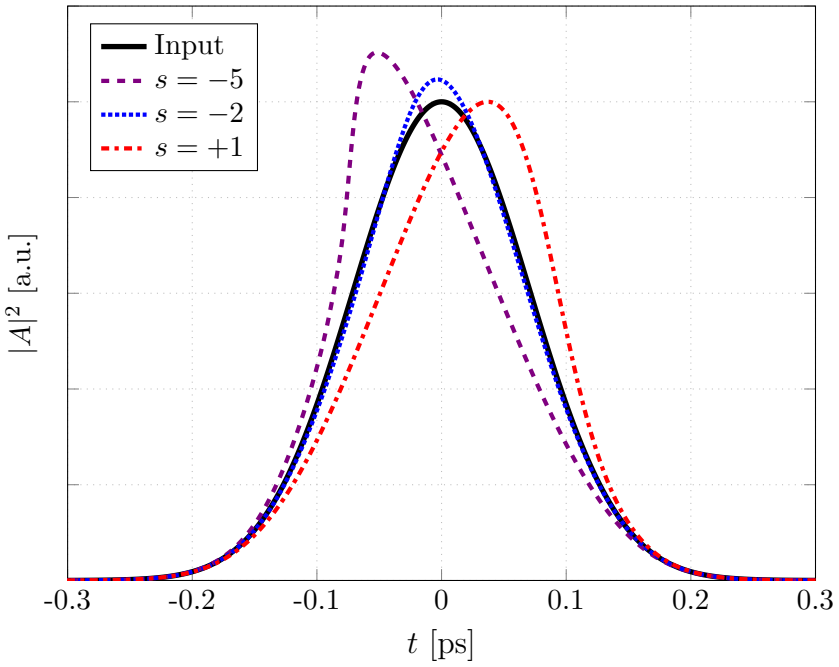

Figure 1. Pulse propagation for $s = -5$ (dashed line), $s = -2$ (dotted line), and $s = 1$ (dash-dotted line). The input pulse is shown with a solid line. No shock-wave formation is observed for $s = -2$. Input pulse: $P_0 = 10$ kW, $\lambda_0 = 1550$. The pulse is propagated 1.5 km along a waveguide with $\gamma_0 = 1$ W^{-1} km^{-1} and no linear dispersion.

Since we are dealing with lossless waveguides the pulse energy does not depend on z. It can be shown that, in the context of Eq. (12) and for even functions $\rho(\tau)$, the delay is governed by the equation (see Appendix C)

$$\frac{\partial T}{\partial z} = \frac{\gamma_0}{2\omega_0}(s+2)P_{\text{eff}}(z), \tag{17}$$

where we have introduced

$$P_{\text{eff}}(z) = \frac{\int_{-\infty}^{+\infty} |A(t,z)|^4 dt}{\int_{-\infty}^{+\infty} |A(t,z)|^2 dt}. \tag{18}$$

Observe that this result agrees with the prediction in the previous section that there is no delay in the case of $s = -2$. Assuming that $P_{\text{eff}}(z)$ does not change significantly with z, then

$$T(z) = (s+2)\frac{\gamma_0 P_{\text{eff}}}{2\omega_0} z. \tag{19}$$

As an example, in the case of *sech* pulses the delay is given by

$$T(z) = \frac{(s+2)}{3}\frac{\gamma_0 P_0}{\omega_0} z. \tag{20}$$

This equation can be used to estimate the value of s by measuring the time delay experienced by an adequate pulse launched into an optical waveguide. Details of this idea were developed in Ref. [48], although the preceding calculations were omitted there. Figure 2 shows and excellent agreement between Eq. (20) and simulation results. These results correspond to the propagation of a 100-fs *sech*-shaped pulse with peak power $P_0 = 2$ kW and central wavelength $\lambda_0 = 1550$ nm. The waveguide is 500-m-long with parameters $\gamma_0 = 1\ \mathrm{W^{-1}\,km^{-1}}$, $\beta_2 = -20\ \mathrm{ps^2\,km^{-1}}$, compatible with those of a standard single-mode optical fiber. As it is discussed in Ref. [48], we are not aware of any direct measurement techniques of the self-steepening parameter in the literature; as such, this is an important result developed on the basis of the pcNLSE.

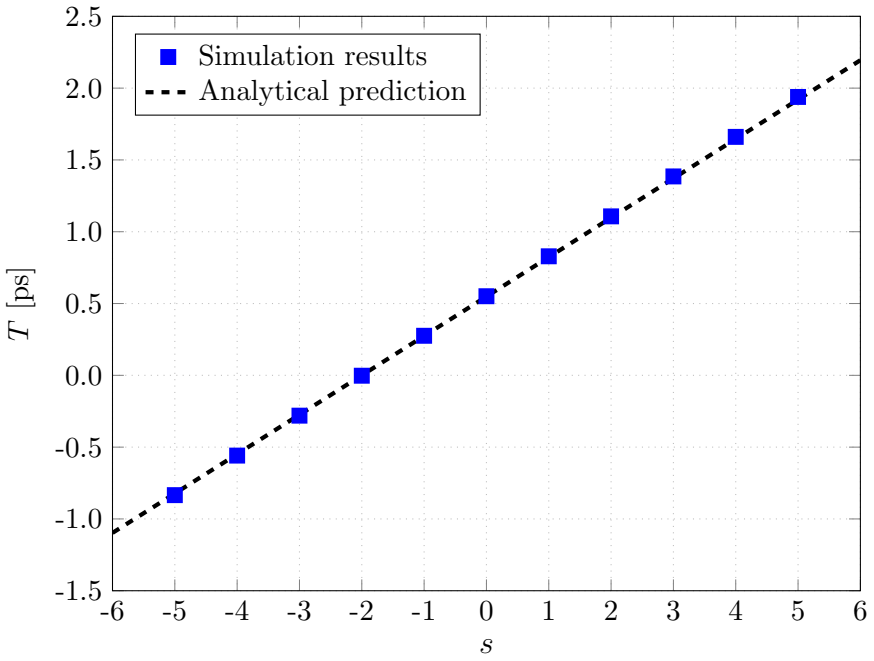

Figure 2. Delay experienced by the pulse as a function of the self-steepening parameter s. There is an excellent agreement between the theoretical prediction (dashed line) and simulation results (squares). A 100-fs *sech*-shaped pulse with $P_0 = 2$ kW and $\lambda_0 = 1550$ nm was propagated along a 500-m-long fiber with $\gamma_0 = 1\ \mathrm{W^{-1}\,km^{-1}}$ and $\beta_2 = -20\ \mathrm{ps^2\,km^{-1}}$.

3. Soliton-like pulses

Solitons in optical waveguides have been studied for several decades (see, e.g., [49–53] and references therein.) In particular, solitons for the nonlinear Schrödinger equation (NLSE), with $\beta_k = 0$ for $k \geq 3$ and $\gamma_1 = 0$, were originally found by Zakharov and Shabat [54] by means of the inverse scattering method. For the sake of reference, let

us write the NLSE in this case as

$$i\frac{\partial u}{\partial \zeta} + \frac{\partial^2 u}{\partial \tau^2} + u|u|^2 = 0, \tag{21}$$

where we have assumed that $\beta_2 < 0$ and used a common normalization of the variables

$$u = N\frac{A}{\sqrt{P_0}},\ \tau = \frac{t}{T_0},\ \zeta = \frac{z}{L_D},\ L_D = \frac{T_0^2}{|\beta_2|},\ N^2 = \frac{\gamma_0 P_0 T_0^2}{|\beta_2|}, \tag{22}$$

with T_0 and P_0 two convenient constants related to the pulse width and power, respectively. Soliton solutions can be found for the case $u(\tau, 0) = N\mathrm{sech}(\tau)$, with integer N, as explained in Satsuma and Yajima [55]. In these cases, N is called the soliton order.

Although it is a well-known fact that solutions of the NLSE do not preserve the number of photons in general [36], it may come as a surprise that solitonic solutions suffer from the same shortcoming. This fact has already been treated by Zheltikov [56]. Figure 3 shows the evolution of solitons of order $N = 3$. A 690-W peak-power pulse at a central wavelength $\lambda_0 = 780$ nm was propagated in a fiber with properties commensurate to those of a commercial photonic crystal fiber [57], that is, $\beta_2 = -3.2$ $\mathrm{ps}^2\,\mathrm{km}^{-1}$ and $\gamma_0 = 105$ 1/W/km. As it can be readily seen on the bottom left panel, *NLSE solitons are unphysical in the sense that the mean number of photons changes as they propagate.*

There are also many soliton solutions in the literature for the NLSE with $\gamma_1 \neq 0$ [58–64]. However, in general these solutions do not necessarily conserve the number of photons. The question now becomes whether the photon-conserving NLSE can sustain soliton-like propagation. Instead of looking for soliton solutions from scratch, by using tools such as the inverse scattering method, we try to find new solitons from old. An immediate example is given by the solitons of the NLSE for the case $s = 1$ where both equations coincide. In the remaining of the paper, we focus on two more interesting examples.

3.1. A special type of nonlinearity

The first example is based on a special form of the frequency dependence of the nonlinearity. Let us assume that $\gamma(\omega) = \gamma_0\omega_0/\omega$, with $\gamma_0 > 0$. It is simple to show that in this case the pcNLSE reduces to

$$\frac{\partial B}{\partial z} = -i\frac{\beta_2}{2}\frac{\partial^2 B}{\partial t^2} + i\sqrt{\gamma_0\omega_0}|B|^2 B, \tag{23}$$

where we have assumed that $\beta_k = 0$ for $k \geq 3$ for the sake of simplicity. Since this equation is formally equivalent to the NLSE with $\gamma_1 = 0$, we can resort to the well-known soliton solutions of the NLSE [51,55] to find B-solitons. Solitons in terms of the electric field envelope A can then be computed from Eq. (7). In Fig. 3 we show the propagation of solitons of order $N = 3$. As it can be observed in the bottom right panel the photon number is conserved, a fact guaranteed by the use of the pcNLSE. It also must be noted that, unlike the standard NLSE solitons, the newly found solitons display an asymmetric shape. This fact is put in evidence in the bottom panels in Fig. 4, were we show the difference between the (squared) amplitudes of NLSE and pcNLSE solitons.

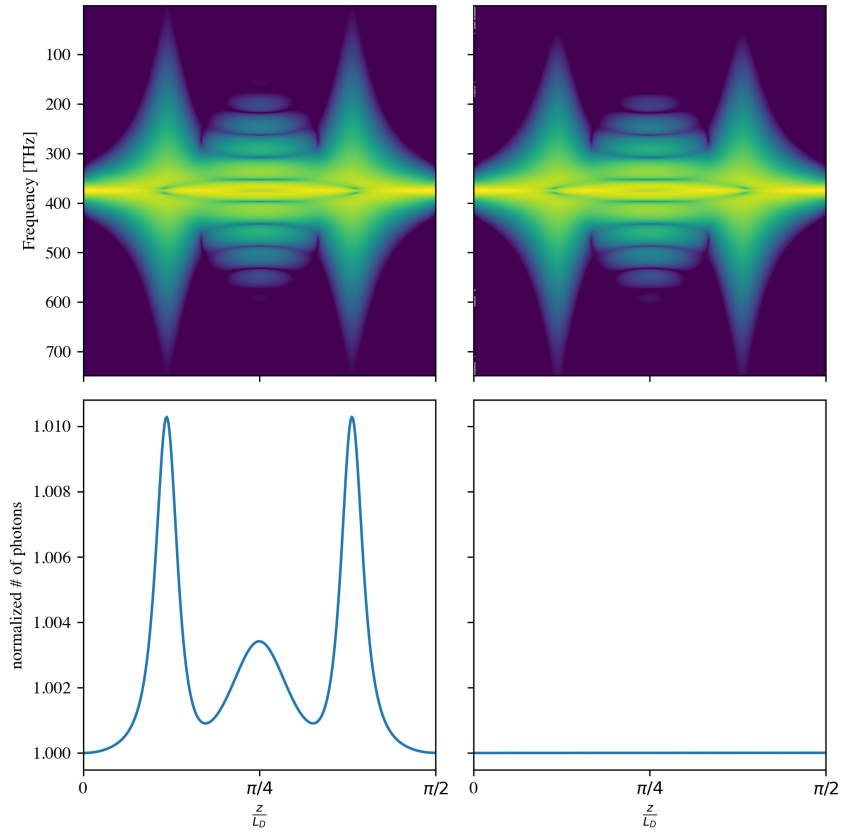

Figure 3. One-period propagation of $N = 3$ solitons for the NLSE (left column) and the pcNLSE (right column). Pulse characteristics: 690-W peak power at $\lambda_0 = 780$ nm. Fiber characteristics for the NLSE soliton: $\beta_2 = -3.2$ ps^2 km^{-1} and $\gamma_0 = 105$ 1/W/km. For the pcNLSE soliton we used $\gamma(\omega) = \gamma_0\omega_0/\omega$. The top row shows the power spectral evolution (darkest is -80 dB with respect to brightest), and the bottom row shows the evolution of the photon number.

Although the frequency profile of the nonlinearity in this example may appear too contrived, to first order in the frequency deviation it can be approximated by $\gamma(\omega) = \gamma_0(1 - \Omega/\omega_0)$. In Fig. 5 we show the evolution of a second-order pcNLSE soliton in a fiber with this type of nonlinearity. This solution preserves the mean photon number, as it is obtained with the pcNLSE, and displays typical higher-order soliton dynamics.

3.2. Approximate Solitons of the B-field

In this section we develop approximate soliton solutions of the pcNLSE for any arbitrary value of the self-steepening parameter. For this purpose, we turn once again to the formal similarity between Eqs. (1) and (11).

Expansion of $\sqrt{(\omega_0 + \Omega)\tilde{\gamma}(\Omega)}$ up to a first order in Ω/ω_0 leads to

$$\frac{\partial \tilde{B}}{\partial z} = i\tilde{\beta}(\Omega)\tilde{B} + i\sqrt{\gamma_0\omega_0}\left(1 + \frac{s+1}{2}\frac{\Omega}{\omega_0}\right)\mathcal{F}\left\{B|B|^2\right\}. \tag{24}$$

In the simple case where $\tilde{\beta}(\Omega) = \beta_2\Omega^2/2$, we may rewrite this equation in the time

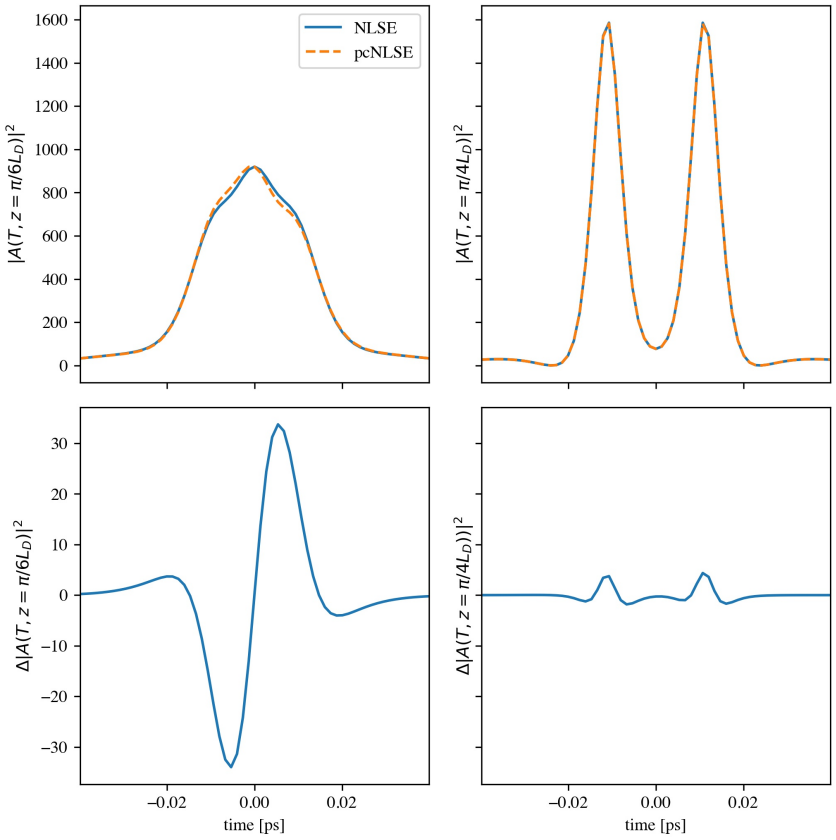

Figure 4. Pulse shape at $z = \pi/6L_D$ and $z = \pi/4L_D$ for an $N = 3$ soliton, and for the NLSE and the pcNLSE (top row). (Botton row) Power difference for the respective top panel. Simulation parameters are the same as in Fig. 3.

domain as

$$\frac{\partial B}{\partial z} = -i\frac{\beta_2}{2}\frac{\partial^2 B}{\partial t^2} + i\sqrt{\gamma_0\omega_0}\left(1 + i\frac{s+1}{2\omega_0}\frac{\partial}{\partial t}\right)\left(B|B|^2\right). \tag{25}$$

Let us assume that $\beta_2 < 0$ and use the following normalization (cf. Eq. (22))

$$u = \frac{NB}{\sqrt{Q_0}},\ Q_0 = \sqrt{\frac{\gamma_0}{\omega_0}}P_0,\ \tau = \frac{t}{T_0},\ \zeta = \frac{z}{L_D},\ L_D = \frac{T_0^2}{|\beta_2|^2},\ N^2 = \frac{\gamma_0 P_0 T_0^2}{|\beta_2|}. \tag{26}$$

Then, we may rewrite Eq. (25) as

$$i\frac{\partial u}{\partial \zeta} + \frac{\partial^2 u}{\partial \tau^2} + \left(1 + i\frac{s+1}{2T_0\omega_0}\frac{\partial}{\partial \tau}\right)\left(u|u|^2\right) = 0. \tag{27}$$

Soliton solutions to this equation were provided by Zhong et al. [64]:

$$u(\zeta, \tau) = V\frac{e^{-\theta} + W^* e^{+\theta}}{\left(e^{-\theta} + We^{+\theta}\right)^2} e^{-\kappa\tau + \frac{(\kappa^2 - \mu^2)}{2}\zeta}, \tag{28}$$

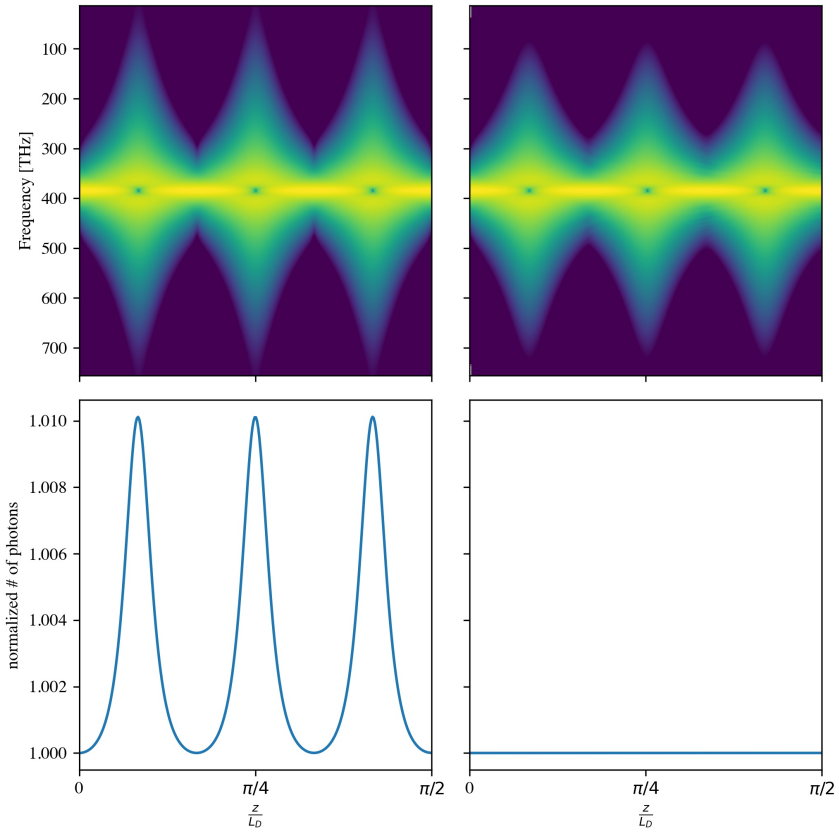

Figure 5. Evolution of a second-order pcNLSE soliton of 1- kW peak power in a fiber with the same parameters as in Fig. 3 but with a nonlinear profile given by $\gamma(\Omega) = \gamma_0(1 - \Omega/\omega 0)$.

where

$$|V|^2 = \frac{4\mu^2}{\sqrt{(1+\kappa S)^2 + (\mu S)^2}}, \qquad W = \frac{1 + kS + i\mu S}{\sqrt{(1+\kappa S)^2 + (\mu S)^2}}, \tag{29}$$

$$\theta = \mu \cdot (\tau + \kappa\zeta), \qquad S = \frac{s+1}{2T_0\omega_0}. \tag{30}$$

and κ and μ are two real-valued parameters.

These equations provide soliton solutions for the approximation to the pcNLSE in Eq. (25). Nonetheless, Fig. 6 shows that these approximate solutions agree well with simulation results with the full pcNLSE even after a propagation length of $10L_D$. Parameters for the fiber are $\gamma_0 = 1\ \mathrm{W^{-1}\,km^{-1}}$, $s = 2$, and $\beta_2 = -25\ \mathrm{ps^2\,km^{-1}}$. The pulse central wavelength is $\lambda_0 = 1550$ nm, $T_0 = 100$ fs, and $P_0 = 10$ kW. For Eqs. (28)-(30) we set $\kappa = 2$ and $\mu = 0$.

4. Conclusions

We have recently introduced a new modeling equation for the propagation of pulses in optical waveguides, the pcNLSE. This equation, unlike the canonical NLSE, guaran-

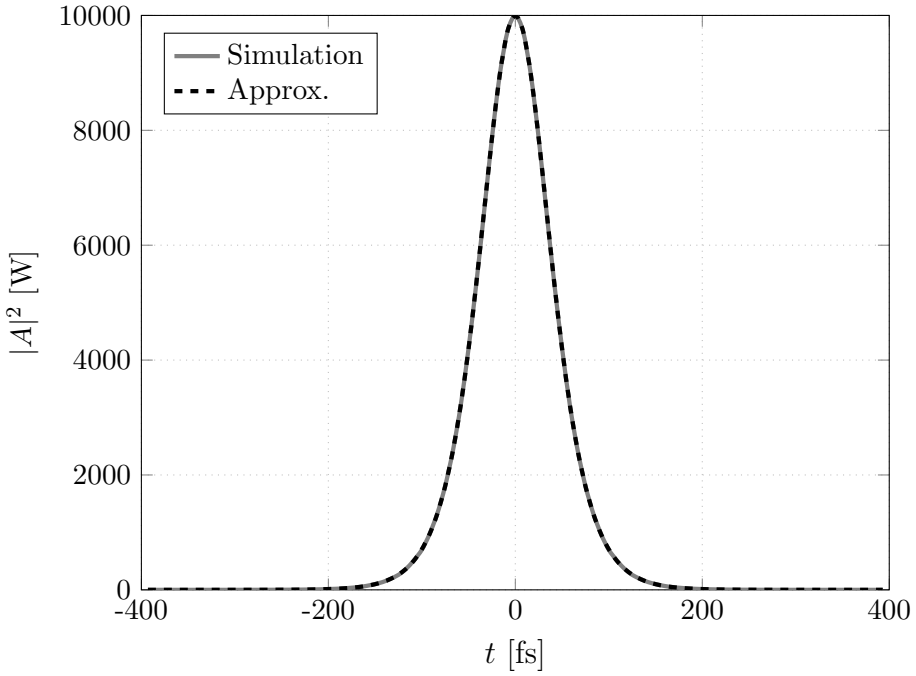

Figure 6. Solitons for $s = 2$: Analytical approximation based on Eq. (24) (black dashed line) and simulation results based on Eq. (11) (solid gray line). A 100-fs pulse with $P_0 = 10$ kW and $\lambda_0 = 1550$ nm was propagated along a $10L_D$-long fiber with $\gamma_0 = 1\ \mathrm{W^{-1}\,km^{-1}}$ and $\beta_2 = -25\ \mathrm{ps^2\,km^{-1}}$.

tees strict conservation of both the energy and the photon number for any frequency-dependent nonlinearity. However, there is still much to be learned about the predictions of this new equation and how they differ from those of the NLSE. In this paper, we tackled this problem by looking at the more familiar case where the sign of the nonlinearity does not change in the wavelength range of interest. Moreover, we focused on a usual linear approximation to the frequency dependence of the nonlinear coefficient.

We showed that, within the approximation of narrowband pulses, the pcNLSE adds a correction term to the NLSE proportional to the squared amplitude and the time derivative of the pulse envelope. Further, the strength of this term is proportional to the deviation of the self-steepening parameter from the photon-conserving condition in the NLSE (see Eq. (12)).

We also described the role of the self-steepening parameter s in two other ways. First, we proved that for $s = -2$ there is no shock-wave formation. Second, we showed that the self-steepening parameter introduces a delay in the propagated pulse. This relation between between the SS parameter and the delay is most relevant as it provides a way to estimate the former from careful measurements of the latter. We must emphasize that this is only possible in the context of the pcNLSE, as the NLSE fails to adequately model the propagation of pulses when $s \neq 1$. Thus, the analytical development in Section 2 provides the basis for a measurement method of the SS parameter which is explored in Ref. [48].

In order to deepen the understanding of the photon-conserving NLSE, we introduced several soliton-like solutions in Section 3. It must be stressed that, unlike NLSE solitons, the solutions put forth in this paper strictly conserve the number of photons.

Finally, although there is much work to be done towards a better understanding of

the pcNLSE, we believe that analyses presented in this paper contribute to gain physical insight into the nonlinear propagation of pulses in waveguides with an arbitrary frequency-dependent nonlinearity.

Appendix A. Approximation for spectrally narrow wavepackets

By expanding the factor multiplying $\tilde{A}(z,\Omega)$ in Eq. (7) in powers of Ω/ω_0, we obtain

$$\tilde{B}(z,\Omega) = \sqrt[4]{\frac{\gamma_0}{\omega_0}}\left(1+\frac{s-1}{4}\frac{\Omega}{\omega_0}\right)\tilde{A}(z,\Omega).$$

From the convolution theorem for Fourier transforms and the fact that $\mathcal{F}\{x^*(t)\} = \tilde{x}^*(-\Omega)$,

$$\begin{aligned}\mathcal{F}\left\{B^*B^2\right\} &= \frac{1}{(2\pi)^2}\iint \tilde{B}^*(-\omega_1)\times\tilde{B}(\omega_2)\times\tilde{B}(\Omega-\omega_1-\omega_2)d\omega_1 d\omega_2 \\ &\approx \sqrt[4]{\frac{\gamma_0^3}{\omega_0^3}}\left(1+\frac{s-1}{4}\frac{\Omega}{\omega_0}\right)\mathcal{F}\left\{A|A|^2\right\} - i\sqrt[4]{\frac{\gamma_0^3}{\omega_0^3}}\left(\frac{s-1}{2}\frac{1}{\omega_0}\right)\mathcal{F}\left\{A^2\frac{\partial A^*}{\partial t}\right\},\end{aligned}$$

where we have kept only terms up to the first order in Ω/ω_0, ω_1/ω_0 and ω_2/ω_0. Let us assume that $|\tilde{A}(\Omega)|$ is significant only when $|\Omega| \ll \omega_0$. In this case,

$$\mathcal{F}\left\{B^*B^2\right\} \approx \sqrt[4]{\frac{\gamma_0^3}{\omega_0^3}}\left[\left(1+\frac{s-1}{4}\frac{\Omega}{\omega_0}\right)\mathcal{F}\left\{A|A|^2\right\} - i\left(\frac{s-1}{2}\frac{1}{\omega_0}\right)\mathcal{F}\left\{A^2\frac{\partial A^*}{\partial t}\right\}\right]. \tag{A1}$$

Moreover, we have

$$\sqrt[4]{(\omega_0+\Omega)^3\tilde{\gamma}(\Omega)} \approx \sqrt[4]{\omega_0^3\gamma_0}\left(1+\frac{s+3}{4}\frac{\Omega}{\omega_0}\right). \tag{A2}$$

We introduce Eqs. (A1)-(A2) in Eq. (10) and keep terms up to the first order in Ω/ω_0 to obtain

$$\begin{aligned}\frac{\partial\tilde{A}}{\partial z} \approx& i\tilde{\beta}(\Omega)\tilde{A} + i\gamma_0\left(1+\frac{s+1}{2}\frac{\Omega}{\omega_0}\right)\mathcal{F}\left\{A|A|^2\right\} \\ &+ \gamma_0\left(\frac{s-1}{2}\frac{1}{\omega_0}\right)\left(1+\frac{s+3}{4}\frac{\Omega}{\omega_0}\right)\mathcal{F}\left\{A^2\frac{\partial A^*}{\partial t}\right\}.\end{aligned}$$

Neglecting the Ω/ω_0^2 term, we have

$$\frac{\partial\tilde{A}}{\partial z} \approx i\tilde{\beta}(\Omega)\tilde{A} + i\gamma_0\left(1+\frac{s+1}{2}\frac{\Omega}{\omega_0}\right)\mathcal{F}\left\{A|A|^2\right\} + \gamma_0\left(\frac{s-1}{2}\frac{1}{\omega_0}\right)\mathcal{F}\left\{A^2\frac{\partial A^*}{\partial t}\right\}.$$

In the time domain this equation reads

$$\frac{\partial A}{\partial z} \approx i\hat{\beta}A + i\gamma_0 \left(1 + i\frac{s+1}{2}\frac{1}{\omega_0}\frac{\partial}{\partial t}\right)\left(A|A|^2\right) + \gamma_0 \left(\frac{s-1}{2}\frac{1}{\omega_0}\right) A^2 \frac{\partial A^*}{\partial t}. \tag{A3}$$

Eq. (12) follows by using the fact that

$$A^2\frac{\partial A^*}{\partial t} = \frac{\partial}{\partial t}(|A|^2 A) - 2|A|^2\frac{\partial A}{\partial t}.$$

Appendix B. The $s = -2$ case

If $s = -2$, Eq. (A3) simplifies to

$$\frac{\partial A}{\partial z} \approx i\hat{\beta}A + i\gamma_0 A|A|^2 + \frac{\gamma_0}{2\omega_0}\frac{\partial}{\partial t}\left(A|A|^2\right) - \frac{3\gamma_0}{2\omega_0}A^2\frac{\partial A^*}{\partial t}.$$

For the sake of simplicity, we assume that there is no linear dispersion, i.e., $\hat{\beta} = 0$. We arrive at Eq. (13) by using the fact that

$$\frac{\partial}{\partial t}(|A|^2 A) = A^2\frac{\partial A^*}{\partial t} + 2|A|^2\frac{\partial A}{\partial t}.$$

In order to prove that the pulse shape does not change, let us return to Eq. (13) to find

$$\begin{aligned} A^*\frac{\partial A}{\partial z} &= +i\gamma_0|A|^4 + \frac{\gamma_0}{\omega_0}|A|^2\left(A^*\frac{\partial A}{\partial t} - A\frac{\partial A^*}{\partial t}\right), \\ A\frac{\partial A^*}{\partial z} &= -i\gamma_0|A|^4 + \frac{\gamma_0}{\omega_0}|A|^2\left(A\frac{\partial A^*}{\partial t} - A^*\frac{\partial A}{\partial t}\right). \end{aligned}$$

These equations lead us to

$$\frac{\partial|A|^2}{\partial z} = A^*\frac{\partial A}{\partial z} + A\frac{\partial A^*}{\partial z} = 0.$$

Appendix C. Time delay

In order to find $\partial_z T$, we need to compute $\partial_z|A|^2$. Using Eq. (12),

$$\begin{aligned} \frac{\partial|A|^2}{\partial z} &= \frac{\partial A}{\partial z}A^* + \frac{\partial A^*}{\partial z}A \\ &= i\left(A^*\hat{\beta}A - A\hat{\beta}^*A^*\right) - \frac{\gamma_0}{\omega_0}\left[A^*\frac{\partial A|A|^2}{\partial t} + A\frac{\partial A^*|A|^2}{\partial t}\right] \\ &\quad - \frac{\gamma_0}{\omega_0}(s-1)|A|^2\left[A^*\frac{\partial A}{\partial t} + A\frac{\partial A^*}{\partial t}\right], \end{aligned}$$

$$\frac{\partial|A|^2}{\partial z} = i\left(A^*\hat{\beta}A - A\hat{\beta}^*A^*\right) - \frac{\gamma_0}{\omega_0}(s+2)|A|^2\frac{\partial|A|^2}{\partial t}$$
$$= i\left(A^*\hat{\beta}A - A\hat{\beta}^*A^*\right) - \frac{\gamma_0}{2\omega_0}(s+2)\frac{\partial|A|^4}{\partial t},$$

where we have used the following simple-to-show relations

$$A^*\frac{\partial A|A|^2}{\partial t} + A\frac{\partial A^*|A|^2}{\partial t} = 3|A|^2\frac{\partial|A|^2}{\partial t},$$
$$\frac{\partial|A|^4}{\partial t} = 2|A|^2\frac{\partial|A|^2}{\partial t}.$$

For the sake of simplicity, let us assume that $\beta_k = 0$ for $k \geq 3$. In this case, we have

$$\frac{\partial|A|^2}{\partial z} = \beta_2 \mathrm{Im}\left(A^*\frac{\partial^2 A}{\partial t^2}\right) - \frac{\gamma_0}{2\omega_0}(s+2)\frac{\partial|A|^4}{\partial t}.$$

Using this result together with Eq. (15) we obtain

$$\frac{\partial T}{\partial z} = \frac{1}{E}\int_{-\infty}^{+\infty} t\frac{\partial|A(t,z)|^2}{\partial z}dt = \frac{1}{E}\int_{-\infty}^{+\infty} t\left[\beta_2 \mathrm{Im}\left(A^*\frac{\partial^2 A}{\partial t^2}\right) - \frac{\gamma_0}{2\omega_0}(s+2)\frac{\partial|A|^4}{\partial t}\right]dt. \quad \text{(C1)}$$

In order to compute the right-hand side of Eq. (C1), we write the pulse envelope as

$$A(z,t) = \sqrt{\frac{P_0T_0}{T_p}}\rho\left(\frac{t-T}{T_p}\right)\exp\left(-iC_p\frac{(t-T)^2}{2T_p^2}\right),$$

where T is the time delay, T_p the pulse width, and C_p the chirp. We have omitted, without any loss of generality, an initial phase. Furthermore, we have assumed that $\int \rho^2(\tau)d\tau = 1$ and hence the pulse energy is conserved and equal to $E = P_0T_0$, where T_0 is the initial pulse width. Moreover, let us assume that $\rho(\tau)$ is an even function. After some algebra, it can be shown that

$$\mathrm{Im}\left(A^*\frac{\partial^2 A}{\partial t^2}\right) = -\frac{C_pP_0T_0}{T_p^3}\left[(t-T)\frac{\partial}{\partial t}\rho^2\left(\frac{t-T}{T_p}\right) + \rho^2\left(\frac{t-T}{T_p}\right)\right].$$

Observe that $\mathrm{Im}\left(A^*\partial_{tt}^2 A\right)$ is even in $(t-T)$. For this reason, we have

$$\int_{-\infty}^{+\infty} t\,\mathrm{Im}\left(A^*\frac{\partial^2 A}{\partial t^2}\right)dt = \int_{-\infty}^{+\infty}(t-T+T)\,\mathrm{Im}\left(A^*\frac{\partial^2 A}{\partial t^2}\right)dt$$
$$= -\frac{\beta_2C_pP_0T_0T}{T_p^3}\left[\int_{-\infty}^{+\infty}(t-T)\frac{\partial}{\partial t}\rho^2\left(\frac{t-T}{T_p}\right)dt + \int_{-\infty}^{+\infty}\rho^2\left(\frac{t-T}{T_p}\right)dt\right].$$

We can integrate by parts the first integral on the second line of this equation:

$$\int_{-\infty}^{+\infty}(t-T)\frac{\partial}{\partial t}\rho^2\left(\frac{t-T}{T_p}\right)dt=-\int_{-\infty}^{+\infty}\rho^2\left(\frac{t-T}{T_p}\right)dt.$$

Thus, we finally have

$$\int_{-\infty}^{+\infty}t\,\mathrm{Im}\left(A^*\frac{\partial^2 A}{\partial t^2}\right)dt=0. \tag{C2}$$

Integrating by parts the second term of Eq. (C1), it can be shown that

$$\int_{-\infty}^{+\infty}t\frac{\partial|A|^4}{\partial t}dt=-\int_{-\infty}^{+\infty}|A|^4dt. \tag{C3}$$

Introducing Eqs. (C2)-(C3) into Eq. (C1),

$$\frac{\partial T}{\partial z}=\frac{\gamma_0}{2\omega_0}(s+2)P_{\mathrm{eff}}. \tag{C4}$$

It is easy to show that

$$P_{\mathrm{eff}}=\alpha_\rho\frac{P_0T_0}{T_p}, \tag{C5}$$

where α_ρ depends on the shape of $\rho(\tau)$. In particular, it is $2/3$ for $\rho(\tau)=\mathrm{sech}(\tau)$ and $1/\sqrt{(}2)$ for $\rho(\tau)=\exp(-\tau^2/2)$. Eq. (19) follows by assuming that T_p does not change significantly with z.

References

[1] Agrawal GP. Nonlinear Fiber Optics. Academic Press; 2012.

[2] Brabec T, Krausz F. Nonlinear optical pulse propagation in the single-cycle regime. Physical Review Letters. 1997;78(17):3282.

[3] Karasawa N, Nakamura S, Nakagawa N, et al. Comparison between theory and experiment of nonlinear propagation for a-few-cycle and ultrabroadband optical pulses in a fused-silica fiber. IEEE Journal of Quantum Electronics. 2001;37(3):398–404.

[4] Kinsler P, New GHC. Few-cycle pulse propagation. Physical Review A. 2003;67(2):023813.

[5] Genty G, Kinsler P, Kibler B, et al. Nonlinear envelope equation modeling of sub-cycle dynamics and harmonic generation in nonlinear waveguides. Optics Express. 2007; 15(9):5382–5387.

[6] Kinsler P. Optical pulse propagation with minimal approximations. Physical Review A. 2010;81(1):013819.

[7] Amiranashvili S, Demircan A. Hamiltonian structure of propagation equations for ultrashort optical pulses. Physical Review A. 2010;82(1):013812.

[8] Amiranashvili S. Hamiltonian framework for short optical pulses. In: New approaches to nonlinear waves. Springer; 2016. p. 153–196.

[9] Amiranashvili S, Radziunas M, Bandelow U, et al. Numerical methods for accurate description of ultrashort pulses in optical fibers. Communications in Nonlinear Science and Numerical Simulation. 2019;67:391–402.
[10] Agranovich VM, Shen YR, Baughman RH, et al. Linear and nonlinear wave propagation in negative refraction metamaterials. Physical Review B. 2004;69(16):165112.
[11] Kourakis I, Shukla PK. Nonlinear propagation of electromagnetic waves in negative-refraction-index composite materials. Physical Review E. 2005;72(1):016626.
[12] Lazarides N, Tsironis GP. Coupled nonlinear Schrödinger field equations for electromagnetic wave propagation in nonlinear left-handed materials. Physical Review E. 2005; 71(3):036614.
[13] Scalora M, Syrchin MS, Akozbek N, et al. Generalized nonlinear Schrödinger equation for dispersive susceptibility and permeability: application to negative index materials. Physical Review Letters. 2005;95(1):013902.
[14] Wen S, Xiang Y, Dai X, et al. Theoretical models for ultrashort electromagnetic pulse propagation in nonlinear metamaterials. Physical Review A. 2007;75(3):033815.
[15] Lægsgaard J. Mode profile dispersion in the generalized nonlinear Schrödinger equation. Optics Express. 2007 Nov;15(24):16110–16123.
[16] Vanvincq O, Travers JC, Kudlinski A. Conservation of the photon number in the generalized nonlinear Schrödinger equation in axially varying optical fibers. Physical Review A. 2011 Dec;84:063820.
[17] Sipe J, Boyd RW. Nonlinear susceptibility of composite optical materials in the Maxwell Garnett model. Physical Review A. 1992;46(3):1614.
[18] Shen H, Cheng B, Lu G, et al. Enhancement of optical nonlinearity in periodic gold nanoparticle arrays. Nanotechnology. 2006;17(16):4274.
[19] Ganeev RA, Ryasnyansky AI. Nonlinear optical characteristics of nanoparticles in suspensions and solid matrices. Applied Physics B. 2006;84(1-2):295–302.
[20] Ryasnyanskiy A, Palpant B, Debrus S, et al. Third-order nonlinear-optical parameters of gold nanoparticles in different matrices. Journal of luminescence. 2007;127(1):181–185.
[21] Falcão-Filho EL, de Araújo CB, Rodrigues Jr JJ. High-order nonlinearities of aqueous colloids containing silver nanoparticles. Journal of the Optical Society of America B. 2007;24(12):2948–2956.
[22] Driben R, Husakou A, Herrmann J. Low-threshold supercontinuum generation in glasses doped with silver nanoparticles. Optics Express. 2009;17(20):17989–17995.
[23] Kim KH, Husakou A, Herrmann J. Linear and nonlinear optical characteristics of composites containing metal nanoparticles with different sizes and shapes. Optics Express. 2010;18(7):7488–7496.
[24] Driben R, Herrmann J. Solitary pulse propagation and soliton-induced supercontinuum generation in silica glasses containing silver nanoparticles. Optics Letters. 2010; 35(15):2529–2531.
[25] Bose S, Chattopadhyay R, Roy S, et al. Study of nonlinear dynamics in silver-nanoparticle-doped photonic crystal fiber. Journal of the Optical Society of America B. 2016 Jun; 33(6):1014–1021.
[26] Zhang H, Hu Z, Ma Z, et al. Anisotropically enhanced nonlinear optical properties of ensembles of gold nanorods electrospun in polymer nanofiber film. ACS Applied Materials & Interfaces. 2016;8(3):2048–2053.
[27] Bose S, Sahoo A, Chattopadhyay R, et al. Implications of a zero-nonlinearity wavelength in photonic crystal fibers doped with silver nanoparticles. Physical Review A. 2016 Oct; 94:043835.
[28] Arteaga-Sierra FR, Antikainen A, Agrawal GP. Soliton dynamics in photonic-crystal fibers with frequency-dependent Kerr nonlinearity. Physical Review A. 2018 Jul;98:013830.
[29] Panoiu NC, Liu X, Osgood RM. Nonlinear dispersion in silicon photonic wires. In: 2008 Conference on Lasers and Electro-Optics and 2008 Conference on Quantum Electronics and Laser Science; IEEE; 2008. p. 1–2.
[30] Panoiu NC, Liu X, Osgood Jr RM. Self-steepening of ultrashort pulses in silicon photonic

nanowires. Optics Letters. 2009;34(7):947–949.
[31] Pendry JB, Smith DR. Reversing light with negative refraction. Physics Today. 2004; 57:37–43.
[32] Wen S, Wang Y, Su W, et al. Modulation instability in nonlinear negative-index material. Physical Review E. 2006;73(3):036617.
[33] Wen S, Xiang Y, Su W, et al. Role of the anomalous self-steepening effect in modulation instability in negative-index material. Optics Express. 2006;14(4):1568–1575.
[34] Xiang Y, Wen S, Dai X, et al. Modulation instability induced by nonlinear dispersion in nonlinear metamaterials. Journal of the Optical Society of America B. 2007;24(12):3058–3063.
[35] Mamyshev PV, Chernikov SV. Ultrashort-pulse propagation in optical fibers. Optics Letters. 1990;15(19):1076–1078.
[36] Blow KJ, Wood D. Theoretical description of transient stimulated Raman scattering in optical fibers. IEEE Journal of Quantum Electronics. 1989;25(12):2665–2673.
[37] Boyd RW. Nonlinear optics, third edition. 3rd ed. Academic Press; 2008.
[38] Bonetti J, Linale N, Sánchez AD, et al. Modified nonlinear Schrödinger equation for frequency-dependent nonlinear profiles of arbitrary sign. Journal of the Optical Society of America B. 2019;36(11):3139–3144.
[39] Linale N, Bonetti J, Sánchez AD, et al. Modulation instability in waveguides with an arbitrary frequency-dependent nonlinear coefficient. Optics Letters. 2020;45(9):2498–2501.
[40] Sánchez AD, Linale N, Bonetti J, et al. Modulation instability in waveguides doped with anisotropic nanoparticles. Optics Letters. 2020;45(11):3119–3122.
[41] Linale N, Bonetti J, Sparapani A, et al. Equation for modeling two-photon absorption in nonlinear waveguides. Journal of the Optical Society of America B. 2020;37(6):1906–1910.
[42] Bonetti J, Linale N, Sánchez AD, et al. Photon-conserving generalized nonlinear Schrödinger equation for frequency-dependent nonlinearities. Journal of the Optical Society of America B. 2020;37(2):445–450.
[43] Dudley JM, Genty G, Coen S. Supercontinuum generation in photonic crystal fiber. Reviews of Modern Physics. 2006;78(4):1135.
[44] Kibler B, Dudley JM, Coen S. Supercontinuum generation and nonlinear pulse propagation in photonic crystal fiber: influence of the frequency-dependent effective mode area. Applied Physics B. 2005;81(2-3):337–342.
[45] Linale N, Grosz DF, Fierens PI. Probing higher-order nonlinearities with ultrashort solitons. In: Frontiers in Optics 2020; OSA; In press.
[46] Marcuse D. RMS width of pulses in nonlinear dispersive fibers. Journal of Lightwave Technology. 1992;10(1):17–21.
[47] Bélanger PA, Bélanger N. Rms characteristics of pulses in nonlinear dispersive lossy fibers. Optics Communications. 1995;117(1-2):56–60.
[48] Linale N, Fierens PI, Bonetti J, et al. Measuring self-steepening with the photon-conserving nonlinear Schrödinger equation. Optics Letters. 2020;45(16):4535–4538.
[49] Hasegawa A, Tappert F, Mollenauer LF, et al. Experimental observation of pico second pulse narrowing and solitons in optical fiber. Applied Physics Letters. 1973;23:142.
[50] Mollenauer LF, Stolen RH, Gordon JP. Experimental observation of picosecond pulse narrowing and solitons in optical fibers. Physical Review Letters. 1980;45(13):1095.
[51] Kivshar YS, Agrawal G. Optical solitons: from fibers to photonic crystals. Academic Press; 2003.
[52] Chen J, Luan Z, Zhou Q, et al. Periodic soliton interactions for higher-order nonlinear Schrödinger equation in optical fibers. Nonlinear Dynamics. 2020;100:2817–2821.
[53] Yang X, Huo D, Hong X. Periodic transmission and control of optical solitons in optical fibers. Optik. 2020;216:164752.
[54] Zakharov VE, Shabat AB. Exact theory of two-dimensional self-focusing and one-dimensional self-modulation of waves in nonlinear media. Soviet Physics JETP. 1972; 34:62.
[55] Satsuma J, Yajima N. B. initial value problems of one-dimensional self-modulation of

nonlinear waves in dispersive media. Progress of Theoretical Physics Supplement. 1974; 55:284–306.
[56] Zheltikov AM. Optical shock wave and photon-number conservation. Physical Review A. 2018;98(4):043833.
[57] Photonics Bretagne. Supercontinuum Photonic Crystal Fiber. Datasheet ; 2020. Available from: https://www.photonics-bretagne.com/wp-content/uploads/2019/09/SUPPCPF-Combined-Spec-Sheet-032019.pdf.
[58] Ohkuma K, Ichikawa YH, Abe Y. Soliton propagation along optical fibers. Optics Letters. 1987;12(7):516–518.
[59] Rangwala AA, Rao JA. Bäcklund transformations, soliton solutions and wave functions of Kaup–Newell and Wadati–Konno–Ichikawa systems. Journal of Mathematical Physics. 1990;31(5):1126–1132.
[60] Chen ZY, Huang NN. Explicit n-soliton solution of the modified nonlinear Schrödinger equation. Physical Review A. 1990;41(7):4066.
[61] Liu SL, Wang WZ. Exact n-soliton solution of the modified nonlinear Schrödinger equation. Physical Review E. 1993;48(4):3054.
[62] Doktorov EV, Shchesnovich VS. Modified nonlinear Schrödinger equation: Spectral transform and n-soliton solution. Journal of Mathematical Physics. 1995;36(12):7009–7023.
[63] Porsezian K, Seenuvasakumaran P, Saravanan K. Next hierarchy of mixed derivative nonlinear Schrödinger equation. Chaos, Solitons & Fractals. 2000;11(14):2223–2231.
[64] Zhong WP, Luo HJ. Limitation of the capacity due to amplified spontaneous emission in a subpicosecond soliton communication system. Chinese Physics Letters. 2000;17(8):577.